1997 ASME Meeting

Dallas, TX, 1997

ASME97-FSI

VORTEX STRUCTURES IN FLOW OVER A RECTANGULAR PLATE

John Sheridan, Kerry Hourigan and Richard Mills
Fluid-dynamics Laboratory for Aeronautical and Industrial Research (FLAIR)
Department of Mechanical Engineering
Monash University
Clayton, Victoria 3168, Australia
Tel: +613 9905 9624, Fax: +613 9905 9639, email:john.sheridan@eng.monash.edu.au

ABSTRACT

Vortex shedding behind plates with rectangular trailing edges and both aerofoil and rectangular leading edges was investigated in a water tunnel. Previous studies, such as that presented by Mills *et al.* (1995), have shown that the base pressure, and hence drag, of such plates can be significantly altered by applying transverse perturbations at certain frequencies. Evidence has been presented to show that this is dependent on the interaction of shed vortices; this study is a first attempt to study the nature of the vortices and how they are influenced by the applied perturbation. This is done by using particle image velocimetry to measure the velocity field close to the plates. From these the vorticity field is derived and its response to perturbation examined. It is shown that the perturbation orders the vorticity field, resulting in increased peak vorticity and circulation in the shed vortices. Thus, their potential for inducing greater suction in the wake has been increased.

NOMENCLATURE

U_∞	free stream velocity (mm/s)
Re	Reynolds number based on plate thickness and U_∞
St	Strouhal vortex shedding frequency
c	chord of plate (mm)
t	thickness of plate (mm)
u'_w	peak wall perturbation velocity (mm/s)
u'	peak perturbation velocity, adjacent to the trailing edge corner of the plate (mm/s)

Introduction

Rockwell (1990) has reviewed separated flows in the context of recent advances in stability theory. He discussed the nature of globally unstable flows and, in particular, addressed the issue of how applied perturbations can affect the vortex shedding and hence pressure fields experienced by the body. The present study concentrates on the particular case of the perturbed flow around rectangular plates, and the effect of the perturbations on the base pressure coefficient and the wake structure.

Nakamura *et al.* (1991) have previously studied separated flows over rectangular plates and proposed that for low Reynolds number (Re < 2000) and chord-to-thickness ratios between 3 and 15, the vortex shedding can be characterised as a shear layer impingement instability, as discussed by Rockwell and Naudascher (1979).

Stokes and Welsh (1986) had previously observed similar results to Nakamura *et al.* at higher Reynolds numbers (15000 - 31000) but where the plates were enclosed in ducts. They found a peak in the duct acoustic resonance amplitude for a particular forcing frequency.

Mills *et al.* (1995) have recently shown how these results can be unified by considering how the peak response (in terms defined by the different investigators) maps on to the frequency - plate length plane. Figure 1 shows the acoustic Strouhal number (based on chord) and chord-to-thickness ratio at which the base pressure coefficient/acoustic resonance/vortex shedding are maximised.

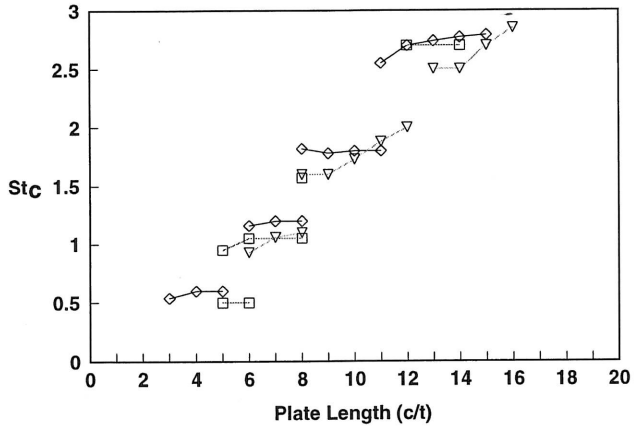

Figure 1: Plot of Acoustic Strouhal numbers (∇) for the present study at which the base pressure drag coefficient is locally a maximum versus c/t. Also shown are the acoustic Strouhal numbers (□) corresponding to peak duct acoustic resonance amplitude from the results of Stokes and Welsh (1986), and the natural Strouhal numbers (◊) from the experiments of Nakamura *et al.* (1991)

From the flow visualisations of Stokes and Welsh (1986), the numerical results of Ohya *et al.* (1992) and the more general discussion by Bearman (1967) of the relationship between base pressure coefficient and vortex formation length, it is clear there is a need for better understanding the way in which vortices form and interact in flow over rectangular plates. This provided the motivation for the present study.

As part of this study, the flow over plates in which the vortices from the leading edge were eliminated was also studied. Figure 2 shows the response of the base pressure to perturbation (applied acoustically, as discussed below) for this case. A large, sharp drop occurs at a critical Strouhal number. While several factors may be responsible for this, including the spanwise coherence as discussed by Wu *et al.* (1993), this study aimed to examine the response of the vortices shed at the trailing edge to such forcing.

Experimental Apparatus and Method

Apparatus

Figure 3 shows a schematic of the low turbulence water tunnel at the CSIRO Division of Building, Construction and Engineering at Highett, which was used for this investigation.

Water was pumped through a diffuser incorporating screens into a settling chamber containing filter material and a honeycomb section. The water then passed through a two dimensional four-to-one contraction with an outlet dimension of 244mm x 244mm, into a duct having the same cross sectional dimensions. There were three sections of the duct. The first section was 660mm long, and was followed by the working section which was

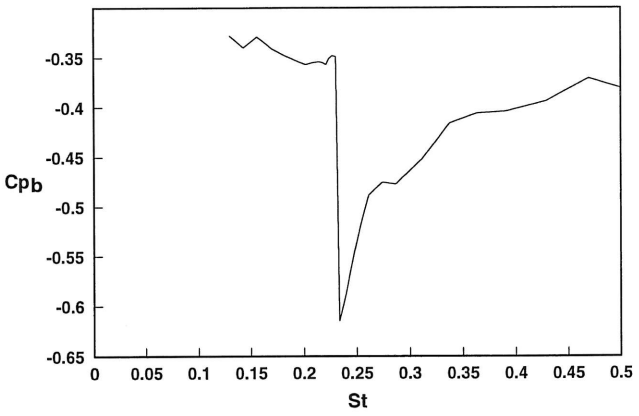

Figure 2: Graph of Cp_b vs St_p for flow past an aerofoil leading edge plate with a 7% velocity perturbation applied.

770mm long, then a 440mm long section which was connected to an outlet reservoir.

The working section had flexibly mounted side walls so that the flow could be perturbed in a direction perpendicular to the mean flow. The two 400mm long moveable side walls had glass windows and was rigidly connected to each other. They were sealed to the remainder of the test section by a thin flexible membrane. Harmonic oscillations of the side walls were produced by a variable speed drive connected to the sidewall support frame via a crank and connecting rod, which enabled a variable stroke. By this means the oscillations of the side walls could be varied from 0 to ±5mm at frequencies between 0 and 6Hz. The wall displacements could be monitored with a Schlumberger DG5 linear displacement transducer. The perturbation velocity (u') measured adjacent to the trailing edge corner of the plates was measured by Wu *et al.* (1993) to be approximately $1.43u'_w$.

A pump driven by an AC electric motor was used to generate the mean flow in the tunnel test section. The maximum velocity achievable in the working section was 400mm/s, and the mean velocity variation measured with a hot film and with PIV measurements was less than ±0.5% of U_∞ across the test section.

For the velocities used in the experiments, the mean longitudinal turbulence level was 0.1% of U_∞ when band-pass filtered between 0.08Hz and 20Hz. The power spectra of the free stream flow showed no distinct spectral peaks within this frequency range. The Reynolds number, based on plate thickness, for all the experiments discussed here was 1000.

Particle Image Velocimetry (PIV)

Instantaneous flow velocities around the models were obtained using a film based PIV technique. The flow was seeded with silver coated hollow glass particles between 10 and 40mm in diameter. The particles are illuminated

using a continuous 4 W Ar-Ion laser spread into a thin sheet, and passed through a side wall of the working section. In order to obtain a usable PIV image, the laser is first passed through a mechanical shutter connected to a 486 PC. The shutter can be controlled to generate laser pulses with minimum periods of 1ms. For all the PIV images acquired, the shutter was pulsed 5 times, with each pulse being 1ms in duration, and 2ms apart.

A 50mm x 50mm plane mirror was used to reflect the image from the working section towards the camera. The mirror was mounted on a General Scanning G325DT Scanner, which was used to rotate the mirror at a constant angular velocity. The axis of rotation was parallel with the sheet of laser light, and perpendicular to the mean flow direction. This allowed a bias velocity to be added to the image in the direction of the mean flow so that all velocities measured from the PIV images were positive. After obtaining a velocity vector field from the image, the bias velocity was simply subtracted from the entire velocity field to obtain the original velocity field. Using this bias velocity technique(based on that developed by the group at Lehigh University, USA), recirculating flows with areas of flow reversal can be studied; any ambiguity regarding flow direction is removed.

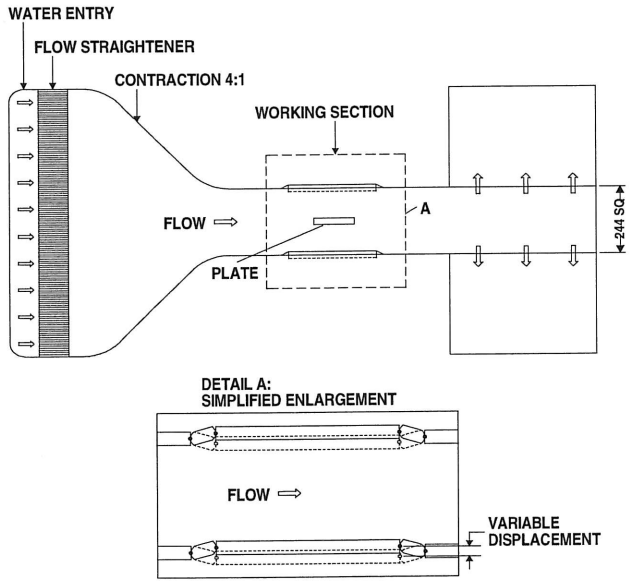

Figure 3: Schematic of the Water Tunnel, showing the working section and the moveable sidewalls.

A 35mm Nikon F90X Single Lens Reflex camera was used to record the PIV images on to Kodak TMax 400 black and white film. Individual PIV images were digitally scanned using a Nikon Coolscan slide scanner, and saved on disk. The images were then processed on a Silicon Graphics work station using in-house software which uses an auto-correlation technique to extract a grid of velocity vectors from the PIV image. Velocity vectors were interpolated in regions with poor data capture rates using linear interpolation between surrounding gridpoints

Results and Discussion

Experiments were conducted on plates with aerofoil leading edges because this isolates the complicating effect of the interaction between the two sets of shed vortices. Given the very sharp reduction in base pressure as the Strouhal frequency approached 0.23, as shown in Fig. 2, it was decided to concentrate on this frequency region to see the effect on the vortices.

Figure 5 shows the velocity field and the vorticity field for flow over the trailing edge of such a plate without perturbation. In the case shown in Fig.4 the flow was perturbed at a Strouhal frequency of 0.25Hz, this being close to the frequency at which the substantial reduction seen in Fig.2 occurred. The amplitude of the perturbation was 7% of the freestream velocity.

While it appears that the perturbation did not affect the wavelength of the vortex shedding, it appears clear, even from the velocity field that there was a more-ordered flow when the perturbation was applied. This is seen even more clearly in the vorticity field; when the perturbation is applied the vortex street is well-ordered but without it there is a degree of disorder. Further evidence of this order is evident in the different levels of peak vorticity for the two cases. When the flow was perturbed the peak vorticity rose from 5.9 (non-dimensionalised with t/U_∞) to 10.3, a 75% increase (see Table1).

It is recognised that the peak vorticity is not the only measure of the "strength" of the vortices but it is considered to be representative enough to show the ordering effect of the perturbation. It will be shown later that there is a degree of consistency in the change in vorticity by examining the vorticity as it varies in the streamwise direction.

It is also important to note here that the change in peak vorticity is a result of *ordering* of the vorticity field in the wake rather than an *increase* of vorticity in the initial boundary layers. The additional vorticity created by such a small perturbation in the boundary layer is negligible and certainly less than the increase in peak vorticity found here.

The increase in peak vorticity will cause a decrease in base pressure of the vortex; however, of itself this may not result in a reduction in the base pressure on the body. Additional factors are the position of the vortex relative to the trailing edge and the spanwise correlation of the vortex shedding. The latter factor has been shown to occur by Wu *et al.* (1993).

When vortices are also shed from the leading edge, e.g. with a rectangular leading edge, these vortices convect along the plate, eventually interacting with those shed at the trailing edge. It is the nature of this interaction which Mills *et al.* (1995) have suggested is the cause of the staged variation in the base pressure coefficient of the

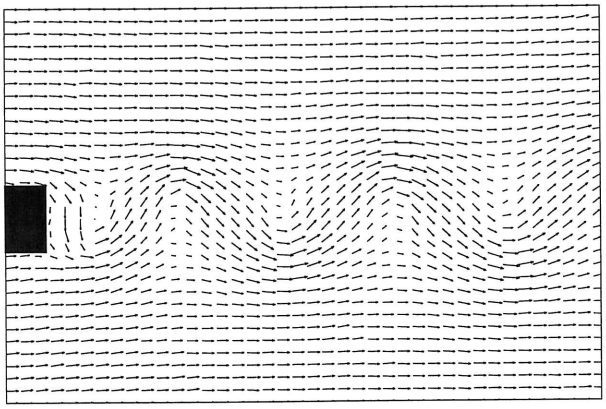

(a)

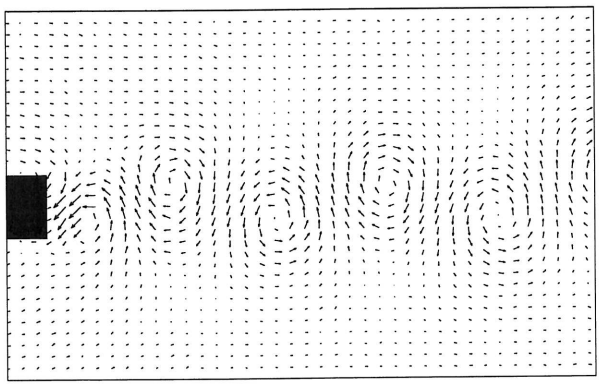

(b)

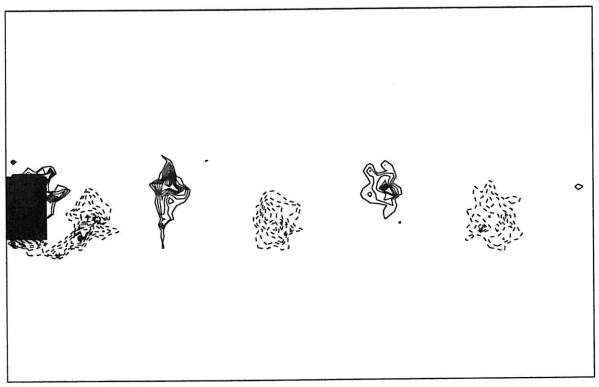

(c)

Figure 4: Velocity vectors behind the trailing edge of an aerofoil leading edge plate of thickness 12.5mm, in the presence of a 7% transverse velocity perturbation with Re=1000, frame of reference: (a) fixed to plate, (b) moving at $0.8U_\infty$, (c) vorticity contour plot

rectangular plate with chord to thickness ratio and applied sound frequency.

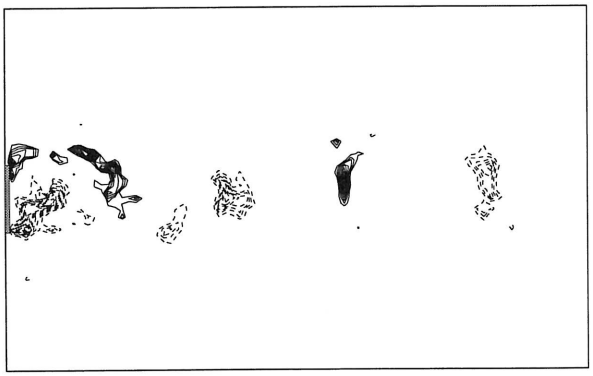

Figure 5: Vorticity plot, aerofoil leading edge, no perturbation

That the vortex shedding at the leading edge also locks on to the applied perturbation can be seen from Fig.6. When perturbed (b) the vorticity, evident in the separating shear layer of (a), rolls up into defined, coherent structures. Previous smoke wire visualisations by Mills *et al.* (1995) have shown that the convection velocity appears independent of the plate length. Thus, the phase relation between the leading and trailing edge vortices when they interact at the trailing edge depends on plate length. The two sets of shed vortices can be additive in that they amalgamate to cause a region of intense low pressure directly behind the trailing edge. Alternatively, the leading edge vortex may arrive at the trailing edge when the formation phase of the trailing edge vortex is such that the arriving vortex is discharged outwards away from the plate. In this case the net effect is a less intense region of low pressure in the wake, and hence the base pressure coefficient is not as low.

Fig. 7 shows the velocity field (a), velocity field with the vortex convection velocity removed (b) and the vorticity field (c). Fig. 8 shows the same data for the case when a 7% perturbation is applied at a frequency of 0.17; this results in a low base pressure coefficient for plates of this chord to thickness ratio (c/t=10).

The effect of the locked on vortex shedding is apparent in the degree of order in the wake; this is particularly evident in the velocity field when the convection velocity is removed. The effect of the applied perturbation on peak vorticity and circulation in the vortices (measured using the method of Wu *et al.* (1994)) is shown in Table 1. The peak vorticity is increased by 60% when the perturbation is applied. As discussed above, it is difficult to make a comparison between the two cases purely on the basis of the peak vorticity of a single vortex in the wake. Fig. 9 shows the vorticity for all cases discussed as a function of streamwise distance. Clearly, the perturbation results in an ordering of the vorticity field.

Case	Circulation	Peak Vorticity
Aerofoil leading edge (no perturbation)	2.17	5.9
Aerofoil leading edge (7% perturbation)	3.21	10.3
Rectangular Plate (no perturbation)	1.21	1.68
Rectangular Plate (7% perturbation)	1.67	3.03

Table 1: Comparison of peak vorticity and circulation in the wake behind different plates.

Conclusions

Several important conclusions can be drawn from the above which help advance our understanding of the flow over rectangular plates and its response to transverse perturbation.

It has been established that when a transverse perturbation is applied to the flow, the vortex shedding at the leading edge and the trailing edge can be locked on to it.
In the absence of leading edge vortices, this can result in vortices rolling up more tightly behind the trailing edge which, in combination with the increase in spanwise coherence found by Wu *et al.* (1993), results in a sharp drop in the base pressure.

When leading edge vortices are present, they also can lock on to the applied perturbation. How the two sets of vortices then interact at the trailing edge depends on their phase relationship, which in turn depends on the phase in the formation cycle of the trailing edge vortex when the leading edge vortex arrives at the trailing edge.

What has been shown here is the potential for increased effect on the base pressure due to the increased ordering of the vortices, resulting in increased peak vorticity.

Work now being undertaken is examining the effect of the perturbation characteristics and the plate length on the vortex interactions in the wake.

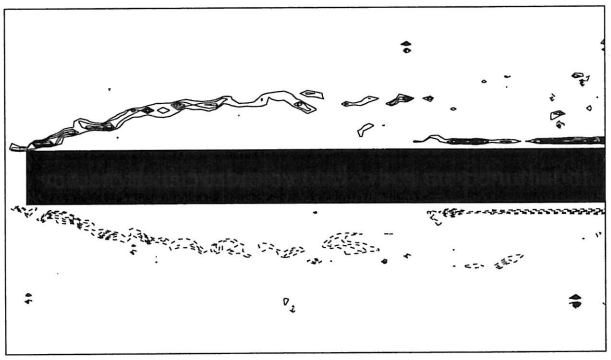

(a)

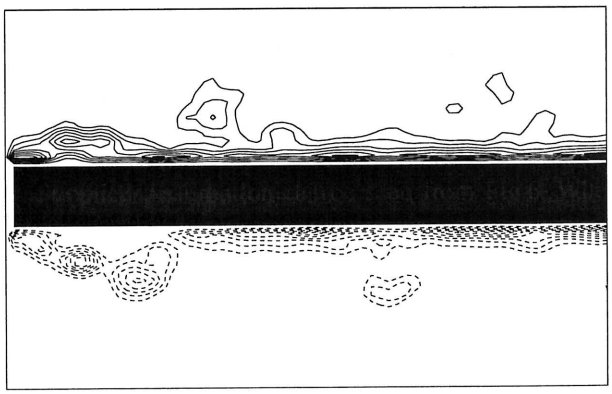

(b)

Figure 6: Vorticity plots for flows over a rectangular plate with c/t=10: (a) no external perturbations applied, (b) 7% transverse velocity perturbation applied.

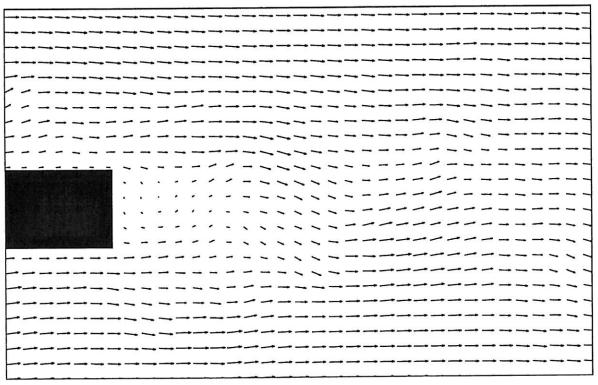

(a)

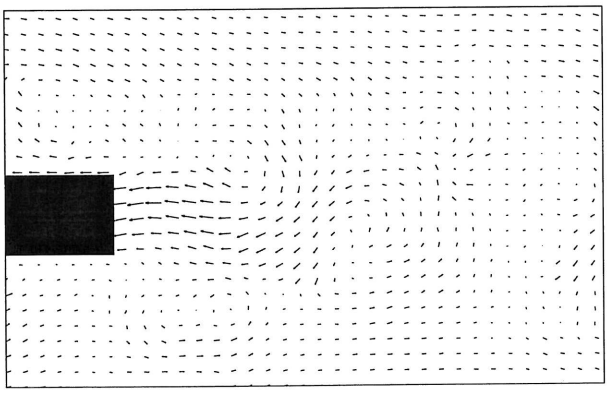

(b)

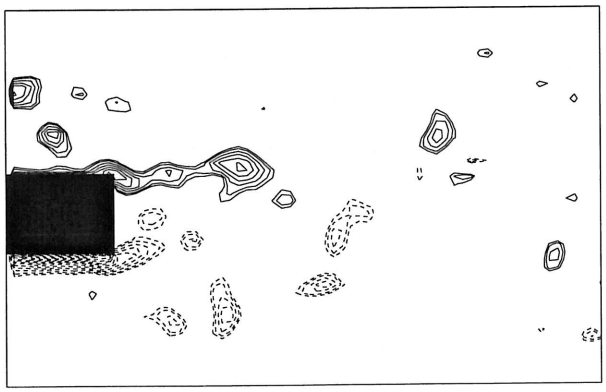

(c)

Figure 7: velocity vector plots in frame of reference of (a) the plate and (b) the convection velocity, and (c) vorticity contours for rectangular plate - no perturbation

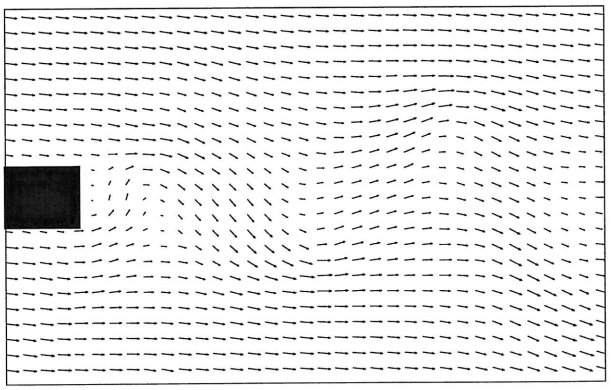

(a)

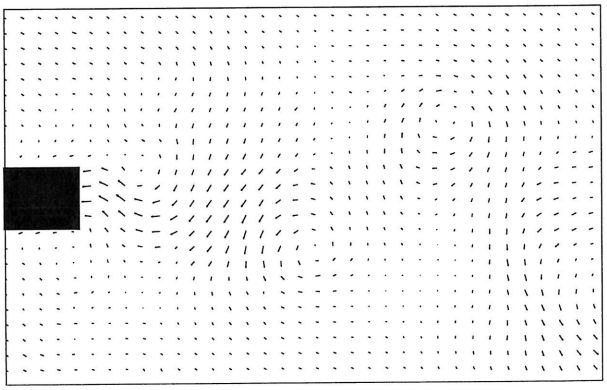

(b)

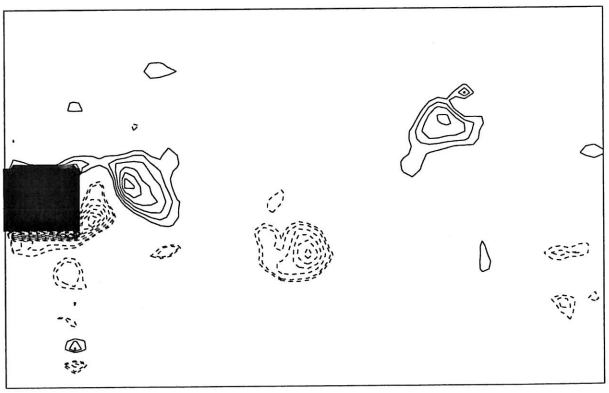

(c)

Figure 8: velocity vector plots in frame of reference of (a) the plate and (b) the convection velocity, and (c) vorticity contours for rectangular plate - with 7% perturbation.

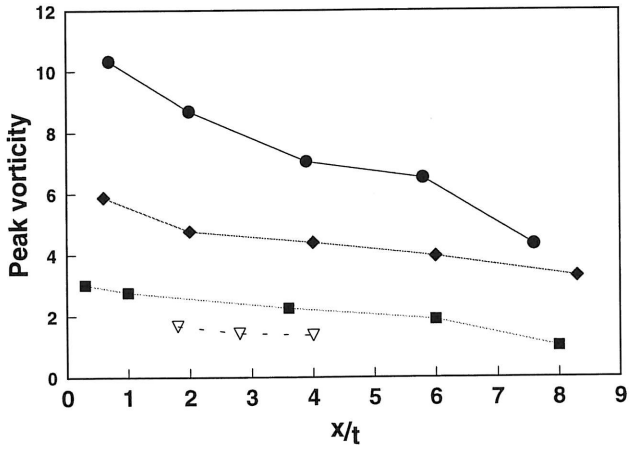

Figure 9: Graph showing the variation of peak vorticity with streamwise distance (x/t) from the trailing edge of different plates (•) aerofoil leading edge with 7% velocity perturbation at St=0.25, (♦) aerofoil leading edge with no perturbation, (■) rectangular plate (c/t=10) with 7% perturbation at St=0.17. (▽) rectangular plate (c/t=10) with no perturbation.

ACKNOWLEDGMENTS

The authors wish to thank Martin Welsh and Wu Jie of the CSIRO for use of facilities and support of the project. They also acknowledge the use of the *PIVFlow* software developed by Dr. N. Lawson of the University of Melbourne.

REFERENCES

Bearman, P.W. 1967 The effect of base bleed on the flow behind a two dimensional model with a blunt trailing edge. *The Aeronautical Quarterly*, **18**, 241-255.

Mills, R., Sheridan, J., Hourigan, K., Welsh, M.C. 1995 The mechanism controlling vortex shedding from rectangular bluff bodies, *12th Annual Australian Fluid Mechanics Conference,* Sydney Australia pp 225-230.

Nakamura, Y., Ohya, Y., and Tsuruta, H. 1991 Experiments on vortex shedding from flat plates with square edges, *J. Fluid Mech.*, **222**, 437-447.

Ohya, Y., Nakamura, Y., Ozono, S., Tsuruta, H. and Nakayam, R. 1992. A numerical study of vortex shedding from flat plates with square leading and trailing edges, *J. Fluid Mech.*, **236**, 445-460.

Rockwell, D. 1990 Active control of globally-unstable separated flows. ASME - Symposium on Unsteady Flows, Toronto.

Rockwell, D. and Naudascher, E. 1979 Self-sustained oscillations of impinging free-shear layers. *Ann. Rev. Fluid Mech.*, **11**, 67-94.

Stokes, A.N. and Welsh, M.C. 1986 Flow-resonant sound interaction in a duct containing a plate, Part II:Square leading edge, *J. Sound and Vibration,* **104**, 55-73.

Wu, J., Sheridan, J., Soria, J., Welsh, M. and Hourigan, K. 1993 Experimental investigation of vortex shedding from a plate: effect of external velocity perturbation *J. Wind Eng. and Ind. Aero.* **49,** 401-410.

Wu, J., Sheridan, J., Soria, J. 1994 An investigation of unsteady flow behind a circular cylinder using a digital PIV method. *ASME FED-Vol..191, Laser Anemometry - Advances and Applications,* 167-172.